
Towards a New in vitro Model of Dry Eye: The ex vivo Eye Irritation Test

Felix Spöler^a · Markus Frenzt^{b,c} · Norbert F. Schrage^{b,c}

^aInstitute of Semiconductor Electronics, RWTH Aachen University, ^bAachen Center of Technology Transfer in Ophthalmology and ^cDepartment of Ophthalmology Aachen University, Aachen, Germany

Abstract

Understanding of dry eye syndrome (DES) today is driven by in vivo analysis of tear osmolarity, tear film break up time, impression cytology and description of symptoms. Existing in vivo models of DES need severe alterations of tear production or corneal integrity. For a more detailed analysis of DES under particular environmental and treatment conditions a considerable lack of in vitro methods exists. The main disadvantage of current in vitro models is the limited experimental time frame of only several hours and the impossibility to evaluate healing of epithelial defects. In the present study, evidence is given that these restrictions can be overcome by modifying the established Ex Vivo Eye Irritation Test (EVEIT) to realize a model system for DES. This test is based on abattoir rabbit eyes allowing an experimental time frame of up to 21 days using self-healing corneal cultures. In first experiments it is demonstrated that different severity levels of dry eye can be simulated in the EVEIT system. High-resolution optical coherence tomography (OCT) is applied to monitor the initial phase of DES under evaporative stress acting on the cornea. We observed changes in corneal layer thicknesses and in scattering properties of the stroma, which are sensitive indicators of environmental stress leading to irritation of the ocular surface under dry eye conditions. The combination of corneal culture under desiccating conditions and OCT monitoring offers a new perspective in understanding and treating of DES and is expected to allow for significant pharmacological screening tests.

Copyright © 2010 S. Karger AG, Basel

The integrity of corneal epithelium depends on a constant supply of healthy tears [1]. Dry eye syndrome (DES) is caused by a deficiency in tear production or an inordinate amount of tear evaporation during the open-eye state, leading to an unstable tear film [2]. Tear fluid deficiency results in weakening of the corneal infection barrier and drying up of the superficial corneal epithelium, which subsequent leads to ocular surface damage and increased risk of sight-threatening corneal infection and ulceration [3–5]. DES is associated with a wide spectrum of symptoms, such as itching, grittiness, pain, blurred vision, and in severe cases visual disability or blindness [6, 7], and represents one of the most frequently established diagnoses in ophthalmology

[8]. A number of epidemiological studies have consistently documented a significant increase in the prevalence of DES with age. The incidence is in the range of 10–33% in the population aged more than 65 years, depending on the structure of the study [9–11]. In addition to age-related DES, air conditioning and low humidity have been identified to be the origin of initial symptoms of DES [12]. Recently, a large-scale survey confirmed reduced health-related quality of life in patients with primary Sjögren's syndrome, expressed by (for example) higher hospitalization rates as well as significantly greater depression and cognitive symptoms when compared to a control group [13].

Because of its high incidence, the accompanying limitations in quality of life and its potentially severe consequences, numerous clinical and experimental studies have been conducted to examine the multifactorial immunopathogenesis and develop appropriate treatment strategies for DES [14–18]. Dry eye animal models play an important role in this research and are applied to study pathogenesis, diagnosis and therapy. Here, mainly in vivo models of rabbits, mice, rats, cats, dogs and monkeys have been developed to mimic the multiplicity of pathophysiological mechanisms involved [2, 5, 19, 20]. Live animal models, which are used to examine quantitative tear film deficiency and environmental stress, use surgical removal, irradiation or closure of the lacrimal gland excretory duct [21–23], prevention of eyelid closure [24], drug-induced suppression of tear secretion [5] and increased tear evaporation in a controlled low-humidity environment [25], optionally supplemented by a reduced blinking frequency induced by physical strain [26].

Since corneal inflammation, for example, induces increased lacrimation [27], changes in the tear secretion or goblet cell secretion (as a reaction to the externally forced dry eye conditions) are likely within these models. These unknown parameters can have an evident effect on the significance of the results obtained [4]. In addition, to achieve statistical certainty in spite of interindividual differences, extensive series of animal experiments have to be performed, which are time-consuming and resource-intensive. Therefore, reliable and highly standardized methods are required to provide economic and logistical advantages. One potential avenue is to replace animal tests by organotypic living models in research and pharmacological tests investigating specific problems in dry eye.

Many intrinsic parameters like immune, endocrine and neuronal factors can only be modeled using living organisms. In contrast, investigation of extrinsic parameters – like generalized quantitative tear film deficiency or environmental stress and treatment modalities addressing these effects – can also be conducted using withdrawn organs and cell or organ cultures. An ex vivo model of dry eye was demonstrated for the first time by Choy et al. [4, 7], using freshly enucleated porcine eyes. Within this model, the variation in mimicked lacrimation and blinking intervals allows for the simulation of dry eye conditions of different levels of severity [28]. This model has already been applied to compare the effects of different artificial tears under simulated dry eye conditions [29]. Evaluation criteria accessible within this model are:

corneal damage (graded by fluorescein staining) and viability of cells in the central and peripheral region of the corneal epithelium (assessed by the trypan blue dye exclusion test after 4 h). Here, the time frame is limited by the increasing mortality rate of cells due to the reduction in their metabolic capabilities in the external environment.

To expand the usable time scale for experiments and to allow for a detailed analysis of corneal regeneration following corneal drying under different treatment conditions, it is feasible to apply corneal cultures as a substitute for the entire bulbi used by Choy et al. [4, 7, 28]. To reach this goal, we intend to integrate the established Ex Vivo Eye Irritation Test (EVEIT) into a model for DES, and in this report we present a feasible method for doing so. Fundamental experiments using time-resolved high-resolution optical coherence tomography (OCT) to investigate the initial behavior of the model under dry eye conditions are presented. Thereby, a detailed insight into the dynamic response of the cornea to different simulated lacrimation intervals is given. To demonstrate the capability of the combination of the introduced dry eye model and OCT examination, we additionally analyzed the effect of artificial tears applied under simulated dry eye conditions.

Materials and Methods

Ex Vivo Eye Irritation Test

The EVEIT allows for the prediction and grading of eye irritation and corrosion in chemical toxicology without the need for animal experiments [30]. This model is based on rabbit corneas slaughtered for food production. It has been proven to react very similarly to human eye tissue concerning behavior during chemical irritation and burn in single and repeated exposures. In a long-term approach, the self-healing system using organ culture methods (derived from human corneal culture) allows for an experimental time frame of up to 21 days. This enables the observation of biochemical and morphological changes after specific chemical exposures, including the evaluation of recovery after chemical or mechanical trauma. The healing process observed after mechanically induced epithelial damage within the EVEIT system is demonstrated in figure 1, using fluorescein staining for follow-up examination.

Engineered corneal tissue constructs tend to have a lack of epithelial integrity, permeability, and mechanical properties of the cornea [31]. The EVEIT system a priori contains the metabolic, functional and anatomical features of the living organ, and therefore there is no need to provide evidence of its similarity to natural cornea. The possibility of evaluating healing after corneal damage in vitro is a unique feature of the EVEIT [30] that will greatly enhance the prediction of pharmacological effectiveness using the intended DES model.

An alternative short-term approach of the EVEIT is performed on whole globes to investigate acute damage and penetration during chemical eye burn limited to a maximum observation period of approximately 6 h. Currently, the EVEIT is being further developed and standardized to meet the requirements for formal regulatory acceptance as a predictor of eye irritation.

Optical Coherence Tomography

In previous studies, it has been demonstrated that OCT is a valuable tool for evaluating morphological changes induced by the treatment conditions being tested and analyzing the process of recovery after chemical trauma within the EVEIT system [32, 33]. Compared to conventional his-

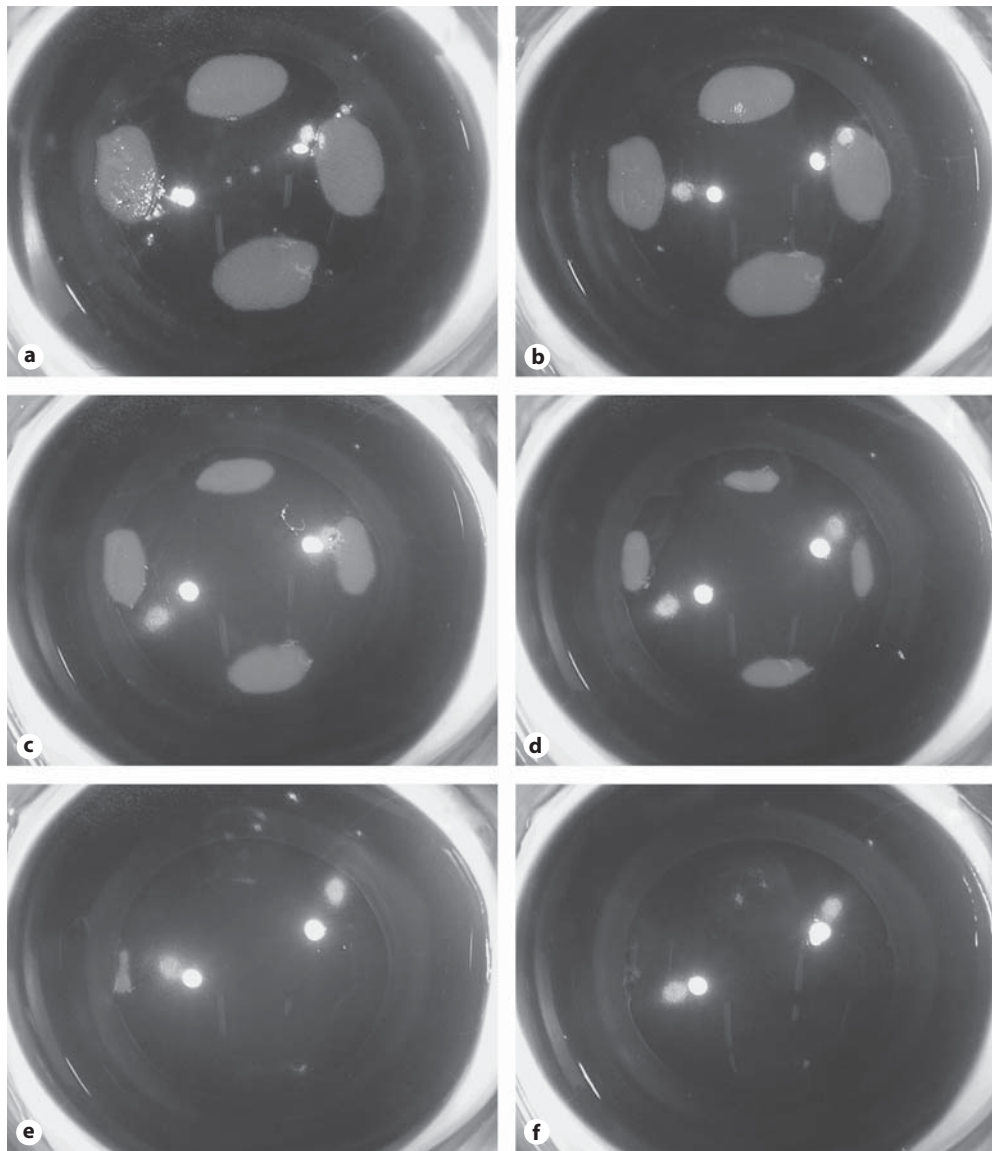


Fig. 1. Documentation of epithelial recovery, observed within the EVEIT system using fluorescein staining. Corneal culture imaged directly after epithelial abrasion in 4 areas, measuring approximately 4 mm² each (a). Images obtained 12 h (b), 24 h (c), 36 h (d), 48 h (e), and 60 h (f) after abrasion to document the healing process.

tological examination, this method enhances process monitoring from static invasive endpoint analysis to real-time dynamic observation. It therefore enables in situ monitoring of the area and the depth of damage, as well as recovery progress over time.

The basic principles of OCT have been extensively discussed elsewhere [34]. Briefly, OCT is the optical analog to medical sonography. For cross-sectional image reconstruction in OCT, near

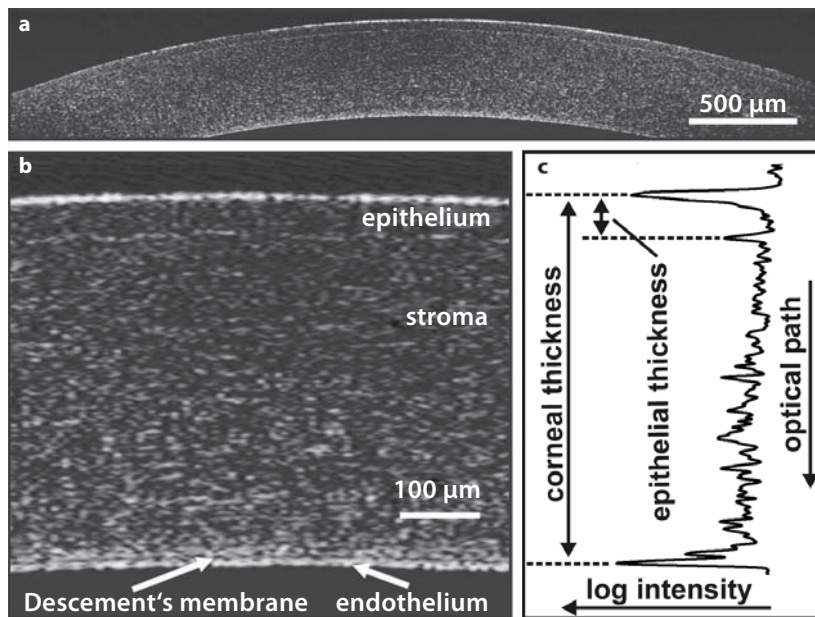


Fig. 2. High-resolution OCT image of an untreated rabbit cornea ex vivo. **a** Overview over the scanned region. $4,500 \times 600 \mu\text{m}$. **b** Magnification of the corneal apex. $600 \times 600 \mu\text{m}$. **c** Logarithmic intensity profile corresponding to **b** given by the average of 10 adjacent A-scans, demonstrating the entrance signals used to derive layer thicknesses.

infrared light (backscattered from structures within the sample) is analyzed by low-coherence interferometry. Hence, a light wave is split into a reference beam with variable path length and a probe beam, which is focused onto the sample. An interference signal is only generated if the path difference of both arms is smaller than the coherence length of the light source. Therefore, the axial resolution in OCT is determined by the coherence length, and consequently by the spectral bandwidth of the employed light source. In analogy to microscopy, the lateral resolution in OCT is determined by the cross-section of the laser beam at the sample site.

The high-resolution OCT system used in this study employs a Ti:sapphire laser oscillator (GigaJet 20, GigaOptics GmbH, Konstanz, Germany) centered at 800 nm as a low-coherence light source. Dispersion management within the laser cavity was deployed to optimize the coherence length of emitted light to $3.6 \mu\text{m}$ in air. The light source emission was coupled into the fiber-based interferometer of a commercial OCT system (Sirius 713, 4optics GmbH, Lübeck, Germany). The latter was modified to support the superior axial resolution specified by the coherence length of the Ti:sapphire laser. Axial and lateral resolutions within tissue were 2.6 and $10 \mu\text{m}$, respectively. The A-scan rate of the OCT system was 50 Hz and the number of data points for each A-scan with an imaging depth of $600 \mu\text{m}$ was 512. A characteristic tomogram of an untreated rabbit cornea monitored by this OCT system is given in figure 2, demonstrating an overview of the scanned region (fig. 2a) and a magnification of the corneal apex (fig. 2b). Here, the epithelial and endothelial layers, the stroma, as well as Descemet's membrane are distinguishable. Ten adjacent A-scans around the center of the image were averaged and plotted in figure 2c, representing the OCT signal amplitude on a logarithmic scale. Layer thicknesses of the cornea can be derived from the distances of the corresponding entrance signals. Here, the repeatability (defined as the standard deviation of

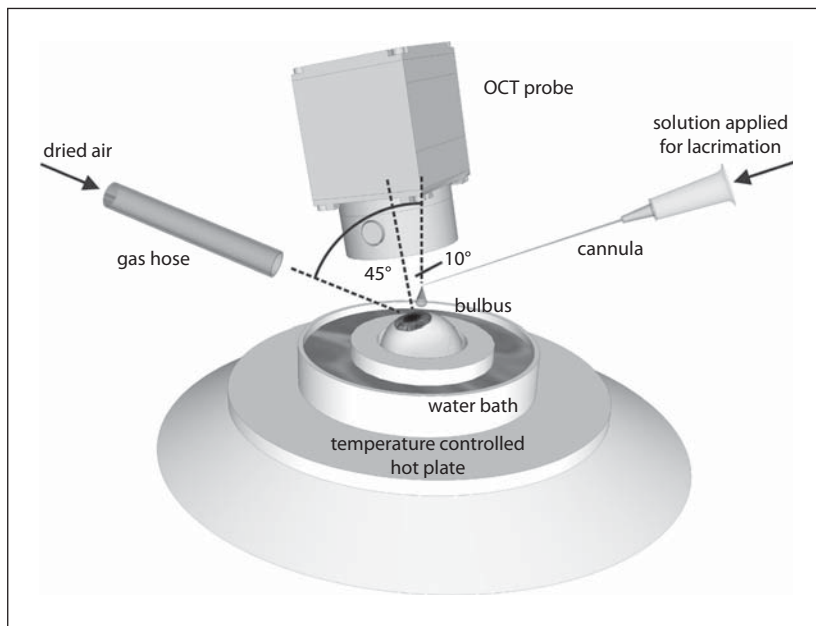


Fig. 3. Experimental setup used to investigate the desiccation of the cornea under simulated dry eye conditions.

the differences obtained in 5 independent and randomized measurements of epithelial thicknesses) was $1.76 \mu\text{m}$, and therefore clearly below the axial resolution of the system.

Experimental Procedure

Within the research project described here, the short-term EVEIT was applied to define appropriate dry eye conditions to model different grades of dry eye. Additionally, the initial phase of corneal drying while simulating different lacrimation intervals and environmental conditions was studied. For this purpose, enucleated white rabbit eyes were used. Rabbit heads were obtained from an abattoir and kept cool until enucleation of the eyes. Only clear corneas without any epithelial defects were processed. All measurements were performed within 12 h after animal death. Excised globes were stored at 4°C within a moist chamber to ensure preservation of the corneal epithelium. Thirty minutes prior to measurements, all eyes were raised to a temperature of 32°C , corresponding to the corneal surface temperature observed in humans [35]. Corneal surface temperature was measured by an infrared thermometer, and was kept constant at $32 \pm 2^\circ\text{C}$ throughout the experiment by immersion of the posterior half of the bulbus into a temperature-controlled water bath (fig. 3). The bulbus was fixed within the water bath by a plastic ring with the cornea face up. Lacrimation was simulated by applying single drops of Ringer's solution ($5.34 \mu\text{l}$) at a defined interval onto the corneal surface. To this end, a cannula connected to a perfusion pump (IPC high-precision multi-channel dispenser, Ismatec, Zürich, Switzerland) was placed above the cornea. By positioning the cannula relative to the cornea, an even distribution of the solution over the corneal epithelium was ensured. To simulate different environmental conditions, the humidity of the ambient air could be reduced by exchange with dried air at variable flow rate. For this purpose, a gas hose with internal diameter of 3.0 mm was used, as illustrated in figure 3. The distance from the nozzle to the corneal apex was 40 mm.

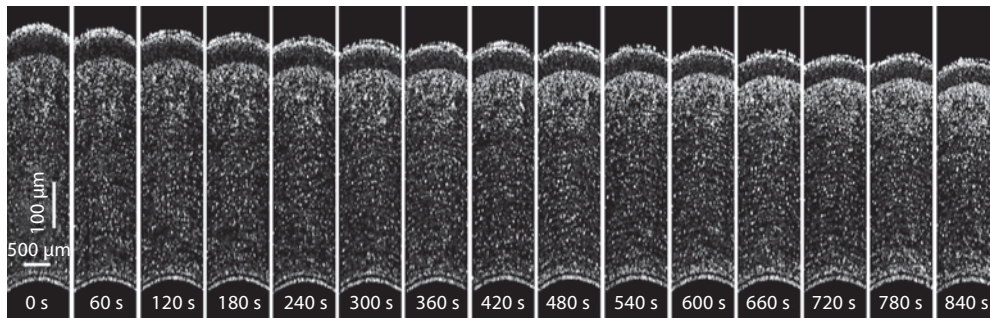


Fig. 4. OCT image sequence, obtained at a lacrimation interval of 60 s and a constant air flow of 2.0 l/min, demonstrating corneal desiccation under simulated dry eye conditions over a time period of 16 min. Each tomogram depicts a cross-sectional image of the cornea at the end of the respective lacrimation interval.

The development of corneal drying and the effect of simulated lacrimation on the corneal epithelium were monitored by OCT imaging with a frame rate of 15 tomograms per minute. The observation period of each run was 16 min, recording a total of 240 tomograms. All OCT measurements within this study were performed on the corneal apex (fig. 3). Tomograms applied for time-resolved measurements were composed of 167 A-scans with a lateral step size of 7 μm . Imaging was started directly after exposure of the cornea to ambient air, defining time point zero. Layer thicknesses of corneal epithelium and of the entire cornea were derived from the optical path lengths in between the corresponding entrance signals of epithelium and stroma on the one hand and epithelium and endothelium on the other hand, as demonstrated in figure 2c. A refractive index of 1.385 was assumed for the conversion of optical to geometrical path lengths [36].

Each experiment within this study was repeated twice, using enucleated eyes of different rabbits. Besides variations in the central corneal thickness of the untreated eyes in the range of $473 \pm 30 \mu\text{m}$ and subsequent deviations in the observed corneal thicknesses during treatment, no significant variations in experimental outcome following identical treatment conditions were observed.

Results

Within our model, both the lacrimation interval and the humidity at the corneal surface can be varied to simulate different severities of dry eye. For the closely related model described by Choy et al. [4], which used enucleated porcine eyes, a lacrimation interval of 60 s is necessary to obtain a significant dry eye effect within a timeframe of 4 h. Here, air flow (not explicitly defined) was applied to increase the rate of evaporation on the corneal surface. To determine the effect of different magnitudes of the air flow, the initial phase of corneal desiccation was monitored by OCT at different flow rates using the short-term EVEIT.

Figure 4 shows a time-series data set obtained at a lacrimation interval of 60 s and a constant air flow of 2.0 l/min. Each tomogram depicts a cross-sectional image of the cornea at the end of the respective lacrimation interval. Two effects of the applied dry

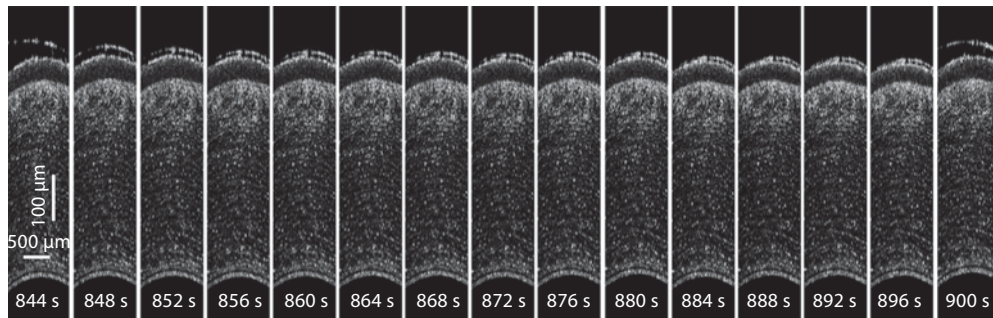


Fig. 5. OCT image sequence, obtained at a lacrimation interval of 60 s and a constant air flow of 2.0 l/min, demonstrating corneal reaction within a single lacrimation interval under simulated dry eye conditions.

eye conditions on the corneal structure can be seen in this time series: first, the corneal thickness decreases continuously with time; second, the OCT signal amplitude of the anterior stroma increases with time. Figure 5 illustrates the OCT images obtained during a single lacrimation interval within the same run depicted in figure 4. The first and the last tomograms within this series were recorded during the simulated lacrimation process, which becomes apparent from the liquid layer depicted on the surface of the epithelium. After application of Ringer's solution onto the corneal epithelium, the thickness of the liquid film decreased over time. However, at the end of the lacrimation interval, the liquid film still had a detectable thickness $>3 \mu\text{m}$. This finding holds true for all lacrimation intervals observed within this run, as is confirmed by the tomograms depicted in figure 4. Another important finding from the analysis of the lacrimation interval in figure 5 is the variation in epithelial thickness. In between 2 wetting procedures, simulating lacrimation at 60-second intervals, a continuous decrease in the layer thickness of the corneal epithelium was observed, whereas a rapid increase was found during the adjacent moistening procedure. A quantitative analysis of these findings is given in figure 6 for 3 runs recorded at different rates of dried air flow over the bulbus. Corneal and epithelial thicknesses were evaluated from the 240 tomograms obtained throughout each experiment and plotted against time. Vertical lines within the graphs define the current moments of corneal wetting as derived from OCT imaging. Here, minor deviations from the interval timer of the perfusion pump can be observed.

In figure 6a, measurements obtained without supplying dried air are analyzed. Measurements depicted in figure 6b and c were conducted at flow rates of 2.0 and 4.0 l/min, respectively. OCT data demonstrated in figures 4 and 5 are included in the diagram presented in figure 6b. In all these experiments, we observed a significant decrease in corneal thickness, which was determined to be 8.0, 16.3 and 44.7% of the initial thickness measured without air flow and flow rates of 2.0 and 4.0 l/min, respectively. Besides the continuous decrease in corneal thickness over time, an oscillation of corneal and epithelial thickness was observed on the timescale of

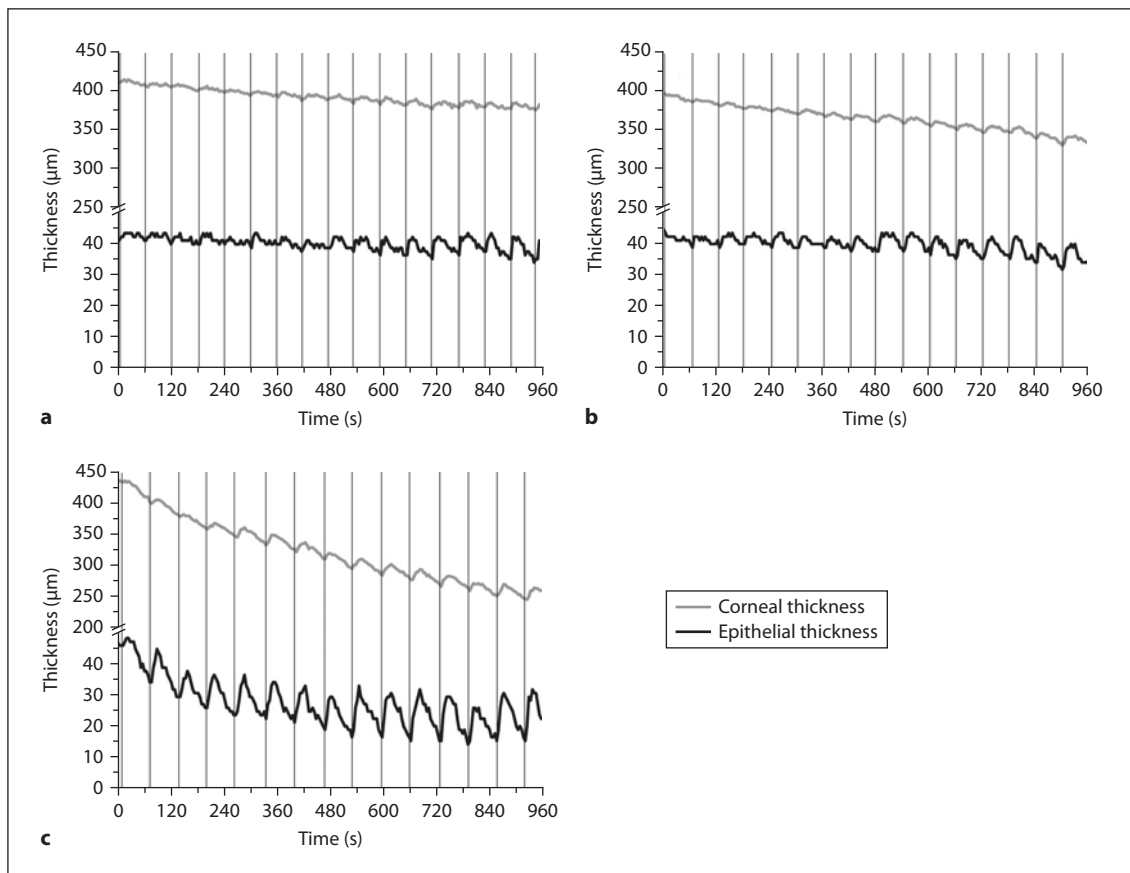


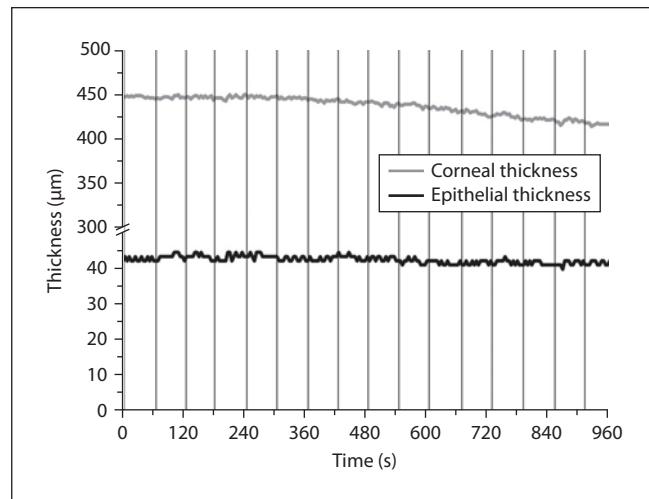
Fig. 6. Temporal development of corneal and epithelial thicknesses under simulated dry eye conditions derived from OCT time series. Vertical lines within the graphs indicate moments of simulated lacrimation. Values taken without supplying dried air (a), and at flow rates of 2.0 (b) and 4.0 l/min (c).

the lacrimation interval of approximately 60 s. Without air flow and with an air flow of only 2.0 l/min, the oscillation builds up during the observation period. Here, its amplitude exceeded the observational accuracy of the layer thicknesses only after 480 and 120 s, respectively.

The effect of artificial tears applied to the model under such simulated dry eye conditions is analyzed in figure 7. For corneal wetting, Hylocare® (Ursapharm GmbH, Saarbrücken, Germany) was used, which replaced Ringer's solution in the experiment depicted in figure 6b. By applying this highly viscous tear replacement solution at a lacrimation interval of 60 s in combination with an air flow of 2.0 l/min, a 6.9% decrease in corneal thickness was observed within 16 min. No variations in epithelial thickness exceeding the observational accuracy were observed within this time span.

To observe the effect of the lacrimation interval on the desiccation of the cornea, it was reduced to 20 s. This value has proven to be suitable to simulate non-desiccating

Fig. 7. Temporal development of corneal and epithelial thicknesses under simulated dry eye conditions (60-second lacrimation interval, 2.0 l/min flow rate of dried air) using artificial tears containing sodium hyaluronate. Vertical lines within the graphs indicate moments of simulated lacrimation.



conditions in the dry eye model of Choy et al. [4]. The air flow was adjusted to 2.0 l/min. Results obtained under these conditions within our system are presented in figure 8. Here, no variations in epithelial thickness exceeding the observational accuracy can be observed. Furthermore, the reduction of corneal thickness observed within 16 min is limited to 2.4% of the initial thickness. This is significantly less than the value of 16.3%, obtained for a lacrimation interval of 60 s under otherwise identical experimental conditions (fig. 6b).

Discussion

In this study, different evaporative conditions and intervals of simulated lacrimation have been studied in order to experimentally induce and treat dry eye symptoms using an in vitro model. High-resolution OCT provides objective information about the initial process of corneal desiccation, with different manifestations in the epithelium and stroma; thus, demonstrating that OCT is a valuable tool to adjust suitable conditions to model different severities of DES.

Time-resolved OCT imaging of corneal desiccation under dry eye conditions show an obvious increase in OCT signal amplitude in the anterior stroma over time, as given in figure 4. The OCT signal amplitude is determined by the scattering cross-section of the tissue under examination, and is therefore defined by its microstructure. Healthy corneal stroma transmits 99% of the incident light without scattering [37]. It is generally accepted that the fibril diameter, the interfibrillar distance and the lattice-like organization of the collagen fibrils play a crucial role in stromal transparency [38]. The observed increase in OCT signal amplitude can therefore be ascribed

to structural changes in the anterior stroma, induced by a water flux to the corneal surface and subsequent stromal drying. This conclusion is supported by the observed decrease in corneal thickness over time. Figure 4 shows that the layer thickness of the tear film on the corneal surface clearly exceeded 3 μm during the entire experiment. As a result, under the applied conditions, corneal desiccation cannot be due to dry spots and evaporation directly on the corneal surface, but has to be accounted for by osmolar forces [39]. Evaporative removal of water from the tear film leads to an increase in osmolarity, and this in turn results in a detectable withdrawal of water from the stroma.

The main source of water in rabbit corneas is the free water within the tissue, which amounts to 76.3% of the corneal weight [40]. Removal of water from the anterior stroma results in increasing concentrations of salts within the cornea, leading to osmolarities of up to 600 mosm/kg measured in DES eyes. Thus, the water flux from the stroma to the corneal surface will decrease with decreasing difference in osmolarity. If the flux becomes too low to compensate for water loss in the epithelium, the epithelial thickness begins to oscillate at the lacrimation frequency, as demonstrated in figures 5 and 6, driven by the osmotic forces of the evaporating tear film. The observed rapid increase and slower decrease in thickness also supports this hypothesis, as a reduction in osmolarity is almost instantaneous when the tear substitute is applied, while evaporative increase in osmolarity is slow. In our model, such osmolar stress delivered to the epithelium was observed only after increased scattering in the anterior stroma was visualized in OCT imaging. Therefore, it can be concluded that water flux from the stroma to the epithelium can initially compensate osmolar desiccation of the epithelium.

The induced continuous change of swelling and shrinking is a membrane-destroying mechanism, resulting in surface damage of biological barriers, which is a typical clinical sign of dry eye, usually observed by fluorescein staining.

Reduced corneal thickness, as observed in our model system, has been assessed as a target variable in dry eye therapy by Karadayi et al. [41]. They documented corneal thicknesses before and after therapy of dry eye patients with tear substitutes. This study confirmed a mean increase in corneal thickness of 29 μm for patients with DES after 2 weeks of therapy. For normal individuals, lacking any symptoms of DES, the mean increase was only 3 μm . Clinical studies on trachomatous dry eyes and on DES have confirmed that corneal thinning is a valuable clinical sign of DES [42, 43]. This fact can easily be incorporated into our dry eye model using OCT for follow-up observation, e.g. in therapeutic studies.

In the normal eye, one third of the tear flow evaporates. However, in dry eye, up to three quarters of the tear film evaporates depending on the distinct pathological entity [44, 45]. Because evaporation accounts for a significant proportion of the tear loss in patients with dry eye, it also plays a crucial role in modeling of DES. Assuming constant temperatures of tear film and surrounding air, the evaporation rate is inversely proportional to relative humidity. This was used to study the influence of

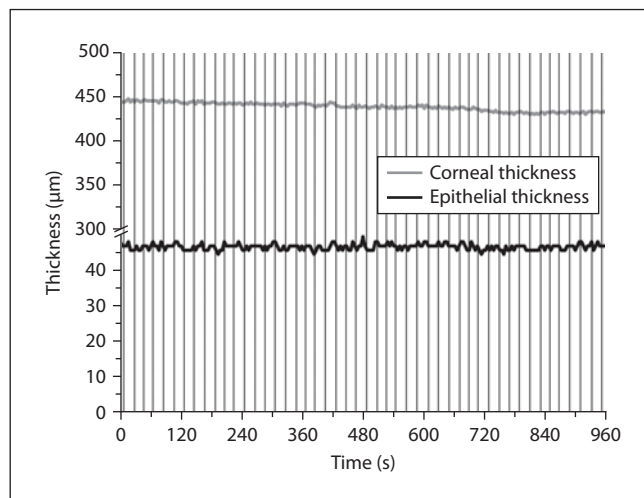
tear evaporation on the initial process of corneal desiccation by applying dried air at different flow rates at the corneal surface (fig. 6). Here, measurements without air flow (fig. 6a) and with an air flow of 2.0 l/min (fig 6b) can be described as combined tear deficient and evaporative dry eye conditions. These are characterized by a preceding desiccation of the anterior stroma and subsequent alternating shrinkage and swelling of the epithelial layer, driven by osmotic forces of the evaporating tear film, as discussed earlier. The higher evaporation rate, which takes place when dried air is applied, only results in quantitative differences concerning the rates of stroma desiccation and corneal shrinkage and is subsequent to the point in time when significant oscillation of the epithelial thickness is observed.

At even higher evaporation rates, the tear film break-up time is less than 60 s, and therefore below the lacrimation interval applied. At an air flow of 4 l/min, tear film break-up time can be estimated from OCT data to be 32 s (not shown here). In this case, epithelial damage is not only driven by osmolar forces, but also by evaporative desiccation of the epithelial cells. This is apparent in the instantaneous and irreversible shrinkage of the epithelial layer observed under these conditions (fig. 6c). Such severe evaporative conditions are not adequate to induce dry eye conditions, and consequently will be avoided in further studies. This is justified by the fact that blinking is especially controlled by ocular surface conditions, resulting in an increased blink rate below the tear film break-up time for dry eye patients with normal corneal sensitivity [46, 47].

Within the first experimental application of our method in pharmacological screening, repeated use of hyaluronate-containing eye drops under simulated severe dry eye conditions was investigated. Application of such a tear replacement solution clearly showed a significant reduction in stained epithelial cells in the trypan blue exclusion test using the porcine dry eye model of Choy et al. [29]. This finding could be reproduced successfully by our model; thus, providing initial confirmation of the applicability of the presented dry eye model in pharmacological tests. It can be concluded from the obtained OCT data that application of this artificial tear replacement prevents the epithelium from being exposed to osmotic stress (fig. 7), while the opposite is observed for application of Ringer's solution as a tear replacement under the same conditions (fig. 6b). Two reasons can be attributed to this finding. First, the water-binding capacity of sodium hyaluronate may increase the water content of the epithelium; second, the high viscosity of the fluid which increases the contact time on the corneal surface.

For use as a negative control, simulation of normal tear film conditions is also important. This is achieved using higher lacrimation rates, as demonstrated in figure 8. Here, stromal desiccation and thereby corneal shrinkage are clearly reduced. In particular, no change in epithelial thickness is observed. Thus, it can be concluded that evaporation within the timeframe of 20 s does not lead to excessive osmolarities of the tear film. Accordingly, no damage to the corneal epithelium induced by osmolar stress is expected under these conditions.

Fig. 8. Temporal development of corneal and epithelial thicknesses under simulated normal conditions (20-second lacrimation interval, 2.0 l/min flow rate of dried air) derived from OCT time series. Vertical lines within the graphs indicate moments of simulated lacrimation.



The results obtained in this preliminary study form a solid basis to further develop the dry eye model introduced here. An important next step will be the transition from the short-term to the long-term approach using the corneal culture system established within the EVEIT. As the time in which the cornea is exposed to dry eye conditions is a key factor for the induced corneal damage, it will be necessary to adapt the environmental conditions for taking this step. For example, it will be necessary to investigate whether a further reduction in the lacrimation interval below 20 s is required to simulate normal conditions over a period of several days. Here, OCT monitoring will be a valuable tool to adjust these conditions, as it supplies not only information about the corneal desiccation, but also gives a detailed insight into the osmotic processes which introduce this stromal and epithelial damage.

Conclusion

There is no doubt that a meaningful in vitro dry eye model will achieve widespread use in order to address scientific problems and develop new treatment strategies and diagnostic approaches for DES. First important steps towards this goal have already been demonstrated within the research project described here, including an applicable corneal culture system, dynamic OCT monitoring of corneal response to the applied dry eye conditions, and adjustable experimental conditions to model different severities of DES. Combining the introduced short-term approach of the dry eye model with the presented corneal culture system will be the next step towards a new and innovative dry eye model. This will allow, for the first time, investigation of the healing processes under simulated dry eye conditions in vitro.

Acknowledgment

We gratefully acknowledge scientific contributions by Stefan Kray and Jaroslav Lazar. This work was partially funded by the Federal Ministry of Education and Research (BMBF), grants 0315491A and 0315491B and by a Pathfinder project within the Exploratory Research Space (ERS) @ RWTH Aachen, grant OPPa71.

References

- 1 Schrage N, Wuestemeyer H, Langefeld S: Do different osmolar solutions change the epithelial surface of the healthy rabbit cornea? *Graefes Arch Clin Exp Ophthalmol* 2004;242:668–673.
- 2 Schrader S, Mircheff AK, Geerling G: Animal models of dry eye. *Dev Ophthalmol* 2008;41:298–312.
- 3 Virtanen T, Konttinen YT, Honkanen N, Härkönen M, Tervo T: Tear fluid plasmin activity of dry eye patients with Sjögren's syndrome. *Acta Ophthalmol Scand* 1997;75:137–141.
- 4 Choy EP, Cho P, Benzie IF, Choy CK, To TS: A novel porcine dry eye model system (pDEM) with simulated lacrimation/blinking system: preliminary findings on system variability and effect of corneal drying. *Curr Eye Res* 2004;28:319–325.
- 5 Dursun D, Wang M, Monroy D, Li DQ, Lokeshwar BL, Stern ME, Pflugfelder SC: A mouse model of keratoconjunctivitis sicca. *Invest Ophthalmol Vis Sci* 2002;43:632–638.
- 6 Terry MA: Dry eye in the elderly. *Drugs Aging* 2001; 18:101–107.
- 7 Choy EP, To TS, Cho P, Benzie IF, Choy CK: Viability of porcine corneal epithelium ex vivo and effect of exposure to air: a pilot study for a dry eye model. *Cornea* 2004;23:715–719.
- 8 Brewitt H, Sistani F: Dry eye disease: the scale of the problem. *Surv Ophthalmol* 2001;45(suppl 2):S199–S202.
- 9 Schein OD, Muñoz B, Tielsch JM, Bandeen-Roche K, West S: Prevalence of dry eye among the elderly. *Am J Ophthalmol* 1997;124:723–728.
- 10 McCarty CA, Bansal AK, Livingston PM, Stanislavsky YL, Taylor HR: The epidemiology of dry eye in Melbourne, Australia. *Ophthalmology* 1998;105: 1114–1119.
- 11 Lin PY, Tsai SY, Cheng CY, Liu JH, Chou P, Hsu WM: Prevalence of dry eye among an elderly Chinese population in Taiwan: the Shihpai Eye Study. *Ophthalmology* 2003;110:1096–1101.
- 12 Wolkoff P, Kjaergaard SK: The dichotomy of relative humidity on indoor air quality. *Environ Int* 2007;33: 850–857.
- 13 Segal B, Bowman SJ, Fox PC, Vivino FB, Murukutla N, Brodscholl J, Ogale S, McLean L: Primary Sjögren's syndrome: health experiences and predictors of health quality among patients in the United States. *Health Qual Life Outcomes* 2009;7:46.
- 14 Kunert KS, Tisdale AS, Stern ME, Smith JA, Gipson IK: Analysis of topical cyclosporine treatment of patients with dry eye syndrome: effect on conjunctival lymphocytes. *Arch Ophthalmol* 2000;118:1489–1496.
- 15 Stern ME, Gao J, Schwalb TA, Ngo M, Tieu DD, Chan CC, Reis BL, Whitcup SM, Thompson D, Smith JA: Conjunctival T-cell subpopulations in Sjögren's and non-Sjögren's patients with dry eye. *Invest Ophthalmol Vis Sci* 2002;43:2609–2614.
- 16 Liu Z, Pflugfelder SC: Corneal surface regularity and the effect of artificial tears in aqueous tear deficiency. *Ophthalmology* 1999;106:939–943.
- 17 Behrens A, Doyle JJ, Stern L, Chuck RS, McDonnell PJ, Azar DT, Dua HS, Hom M, Karpecki PM, Laibson PR, Lemp MA, Meisler DM, Del Castillo JM, O'Brien TP, Pflugfelder SC, Rolando M, Schein OD, Seitz B, Tseng SC, van Setten G, Wilson SE, Yiu SC: Dysfunctional tear syndrome: a Delphi approach to treatment recommendations. *Cornea* 2006;25:900–907.
- 18 Foulks GN: The correlation between the tear film lipid layer and dry eye disease. *Surv Ophthalmol* 2007;52:369–374.
- 19 Barabino S, Dana MR: Animal models of dry eye: a critical assessment of opportunities and limitations. *Invest Ophthalmol Vis Sci* 2004;45:1641–1646.
- 20 Zhu L, Shen J, Zhang C, Park CY, Kohanim S, Yew M, Parker JS, Chuck RS: Inflammatory cytokine expression on the ocular surface in the Botulinum toxin B induced murine dry eye model. *Mol Vis* 2009;15:250–258.
- 21 Helper LC, Magrane WG, Koehm J, Johnson R: Surgical induction of keratoconjunctivitis sicca in the dog. *J Am Vet Med Assoc* 1974;165:172–174.
- 22 Hakim SG, Schroder C, Geerling G, Lauer I, Wedel T, Kosmehl H, Driemel O, Jacobsen HC, Trenkle T, Hermes D, Sieg P: Early and late immunohistochemical and ultrastructural changes associated with functional impairment of the lachrymal gland following external beam radiation. *Int J Exp Pathol* 2006;87:65–71.

- 23 Gilbard JP, Rossi SR, Gray KL, Hanninen LA, Kenyon KR: Tear film osmolarity and ocular surface disease in two rabbit models for keratoconjunctivitis sicca. *Invest Ophthalmol Vis Sci* 1988;29:374–378.
- 24 Fujihara T, Nagano T, Nakamura M, Shirasawa E: Lactoferrin suppresses loss of corneal epithelial integrity in a rabbit short-term dry eye model. *J Ocul Pharmacol Ther* 1998;14:99–107.
- 25 Fabiani C, Barabino S, Rashid S, Dana MR: Corneal epithelial proliferation and thickness in a mouse model of dry eye. *Exp Eye Res* 2009;89:166–171.
- 26 Nakamura S, Shibuya M, Nakashima H, Hisamura R, Masuda N, Imagawa T, Uehara M, Tsubota K: Involvement of oxidative stress on corneal epithelial alterations in a blink-suppressed dry eye. *Invest Ophthalmol Vis Sci* 2007;48:1552–1558.
- 27 Drummond PD: Lacrimation and cutaneous vasodilatation in the face induced by painful stimulation of the nasal ala and upper lip. *J Auton Nerv Syst* 1995;51:109–116.
- 28 Choy EP, Cho P, Benzie IF, Choy CK: Dry eye and blink rate simulation with a pig eye model. *Optom Vis Sci* 2008;85:129–134.
- 29 Choy EP, Cho P, Benzie IF, Choy CK: Investigation of corneal effect of different types of artificial tears in a simulated dry eye condition using a novel porcine dry eye model (pDEM). *Cornea* 2006;25:1200–1204.
- 30 Frenzt M, Goss M, Reim M, Schrage NF: Repeated exposure to benzalkonium chloride in the Ex Vivo Eye Irritation Test (EVEIT): observation of isolated corneal damage and healing. *Altern Lab Anim* 2008;36:25–32.
- 31 Berry M, Radburn-Smith M: Ocular toxicology in vitro – cell based assays. *ALTEX* 2006;23(suppl):313–317.
- 32 Spöler F, Först M, Kurz H, Frenzt M, Schrage NF: Dynamic analysis of chemical eye burns using high-resolution optical coherence tomography. *J Biomed Opt* 2007;12:041203.
- 33 Spöler F, Frenzt M, Först M, Kurz H, Schrage NF: Analysis of hydrofluoric acid penetration and decontamination of the eye by means of time-resolved optical coherence tomography. *Burns* 2008;34:549–555.
- 34 Fercher AF, Drexler W, Hitzenberger CK, Lasser T: Optical coherence tomography – principles and applications. *Rep Prog Phys* 2003;66:239–303.
- 35 Schrage NF, Flick S, von Fischern T, Reim M, Wenzel M: Temperature changes of the cornea by applying an eye bandage. *Ophthalmologie* 1997;94:492–495.
- 36 Drexler W, Hitzenberger CK, Baumgartner A, Findl O, Sattmann H, Fercher AF: Investigation of dispersion effects in ocular media by multiple wavelength partial coherence interferometry. *Exp Eye Res* 1998;66:25–33.
- 37 Meek KM, Leonard DW: Ultrastructure of the corneal stroma: a comparative study. *Biophys J* 1993;64:273–280.
- 38 Meek KM, Boote C: The organization of collagen in the corneal stroma. *Exp Eye Res* 2004;78:503–512.
- 39 Mishima S, Maurice DM: The effect of normal evaporation on the eye. *Exp Eye Res* 1961;1:46–52.
- 40 von Fischern T, Lorenz U, Burchard WG, Reim M, Schrage NF: Changes in mineral composition of rabbit corneas after alkali burn. *Graefes Arch Clin Exp Ophthalmol* 1998;236:553–558.
- 41 Karadayi K, Ciftci F, Akin T, Bilge AH: Increase in central corneal thickness in dry and normal eyes with application of artificial tears: a new diagnostic and follow-up criterion for dry eye. *Ophthalmic Physiol Opt* 2005;25:485–491.
- 42 Guzey M, Satici A, Karadede S: Corneal thickness in trachomatous dry eye. *Eur J Ophthalmol* 2002;12:18–23.
- 43 Liu Z, Pflugfelder SC: Corneal thickness is reduced in dry eye. *Cornea* 1999;18:403–407.
- 44 Mathers WD, Daley TE: Tear flow and evaporation in patients with and without dry eye. *Ophthalmology* 1996;103:664–669.
- 45 Goto E, Matsumoto Y, Kamoi M, Endo K, Ishida R, Dogru M, Kaido M, Kojima T, Tsubota K: Tear evaporation rates in Sjögren syndrome and non-Sjögren dry eye patients. *Am J Ophthalmol* 2007;144:81–85.
- 46 Nakamori K, Odawara M, Nakajima T, Mizutani T, Tsubota K: Blinking is controlled primarily by ocular surface conditions. *Am J Ophthalmol* 1997;124:24–30.
- 47 Nally L, Ousler GW, Emory TB, Abelson MB: A correlation between blink rate and corneal sensitivity in a dry eye population. *Invest Ophthalmol Vis Sci* 2003;44:E-abstract 2488.

Dr. rer. nat. Felix Spöler
 Institute of Semiconductor Electronics, RWTH Aachen University
 Sommerfeldstrasse 24
 52074 Aachen (Germany)
 Tel. +49 241 80 27896, Fax +49 241 80 22246, E-Mail spoeler@iht.rwth-aachen.de